THE FUNCTION OF NANO LAYER IN ENHANCING THE THERMAL CONDUCTIVITY OF TiO_2/WATER NANOFLUIDS

Xiaoyan HUANG [a,b], ***Xiaohui ZHANG*** [a,b,*], ***Shan QING*** [a,b,]

[a]Faculty of Metallurgical and Energy Engineering, Kunming University of Science and Technology, Kunming 650093, China

[b]National local Joint Engineering Research Center of Energy Saving and Environmental Protection Technology in Metallurgy and Chemical Engineering Industry, Kunming University of Science and Technology, Kunming 650093, China

[*] Corresponding author. E-mail address: xiaohui.zhang@kust.edu.cn

Abstract: Nanoparticles have the capability to effectively improve the thermal conductivity of base fluids, thus improving the heat transfer coefficient of heat transfer systems. In this study, a non-equilibrium molecular dynamics (NEMD) method based on the Fourier law is employed to study the thermal conductivity of TiO_2 (r-TiO_2)/water nanofluids with temperatures ranging between 303K and 333K and volume fractions in the range of 1-2%. The ordered layer structure as a shell is analyzed and its influence is surveyed by calculating the number density and radial distribution function (RDF). The results revealed that a clear, solid-like nanolayer of about 0.5 nm can be observed around the nanoparticle. In this regard, the thickness of the nanolayer is less affected by variations in volume fraction and temperature. The g(r) values and the number density decreased with the increase in temperature. Additionally, the g(r) values and the number density at the level of the nanolayer were much higher compared to those at other parts. This indicates the existence of more water molecules in the nanolayer, thereby reducing contact thermal resistance and improving thermal conductivity. Macroscopically, the thermal conductivity increases with the increase in volume fraction. It was found that the increase in the volume fraction from 1% to 2% at 303 K resulted in an increase in the effective thermal conductivity from 1.027 and 1.042, respectively. In other words, the thermal conductivity of the nanofluid was 2.7% and 4.2% higher than that of the base liquid under the same conditions.

Keywords: *Nanofluids, thermal conductivity, microscopic parameters, interfacial layer, nanolayer thickness.*

[*] Corresponding author. Tel.: +86 18487319560

E-mail address: xiaohui.zhang@kust.edu.cn (Xh. Zhang).

1. Introduction

Nanofluids are generally characterized as suspensions with nanoparticles dispersed in heat transfer fluids. Due to their excellent thermophysical properties, they have been widely used in various engineering applications, including electronic device cooling systems [1, 2], grinding [3], solar heating, and other heat transfer processes [4]. They exhibited rapid development, providing a new approach to enhancing the heat transfer coefficient of conventional liquids [5, 6]. Thus, nanofluids can be considered the next generation of heat transfer fluids [7]. The rapid growth in research dealing with nanofluids, including the application areas and different nanofluid types [8, 9], has seen a dramatic increase, especially in the past decade [10-12].

Thermal conductivity is considered a key factor during the heat transfer process in nanofluid applications. Since the thermal conductivity of nanofluids is a direct reflection of the thermal properties of this new generation of heat transfer mediums, they are a hot research topic [13] and have been studied on a wide scale [14]. The major parameters contributing to the enhancement of nanofluids' thermal conductivity are the particle volume fraction, the size and shape of the nanoparticles, and the aspect ratio. In addition, the thermal conductivity of a nanofluid increases with the increase in the nanoparticle's thermal conductivity (considering different types of nanoparticles), particle volume fraction [15, 16] solution pH [17], and system temperature [18].

Based on the previous review and discussion [15-20], it is noted that the effects of volume fraction or temperature on the thermal conductivity of TiO_2 nanofluids have been dealt with from a macroscopic perspective. In this regard, corresponding results can be obtained through experiments. However, heat conduction is a microscopic process that cannot be observed or fully characterized by experiments. Some studies have shown that one of the major mechanisms exhibited in relation to the abnormally enhanced thermal conductivity of nanofluids is the ordered arrangement of liquid molecules on the surface of nano particles [21-24]. This ordered layer structure as a shell at nano particles surfaces is commonly known as the interfacial layer, which was first reported and characterized by Choi et al. [25]. It was shown that the thickness of the interfacial layer plays an intriguing role in heat transmission from nano particles to the base liquid [21]. However, the interface layer is still very difficult to characterize by experiments because of its extremely small size. To address this, some researchers tried to use molecular dynamics (MD) simulations to investigate and evaluate the interfacial layer's effect on the abnormal thermal conductivity.

In their work, Li et al. [22, 26] investigated an argon thin layer of about 0.5nm around copper nanoparticles using MD. Based on the evaluation conducted, they reported the effect of the interfacial layer on the thermal conductivity of the nanofluid. This thin interfacial layer will move with the Brownian motion of the copper nanoparticles and water molecules. The investigations also found that the number density is proportional to the diameter of the nanoparticles, which therefore leads to a significant enhancement of the Cu-Ar nanofluid's thermal conductivity. In connected studies, Wang et al. [27] investigated the thickness and thermal conductivity of the interfacial layer around the nanoparticle in Cu-Ar nanofluids employing equilibrium molecular dynamics (EMD) simulations. They found that the nano-scale thin interfacial layer is characterized by a more ordered structure and a higher thermal

conductivity t compared to the base fluids. In their study, Jin et al. [28, 29], examined the thermal conductivity of different metal/water nanofluids using MD methods. The results indicated that the Au/water nanofluid has a higher thermal conductivity and a thicker nanolayer due to the stronger interaction between gold and water molecules (ε =1.256 kcal·mol^{-1}, σ=2.895 Å). The authors also studied the effects of different surface materials and core-shell ratios on the thermal conductivity of nanofluids. It was shown that, the thermal conductivity of core-shell nanofluids can be significantly enhanced compared to that of heat transfer fluids. The studies reviewed here demonstrate that, MD methods serve as a very effective approach to studying and examining nanolayer structures.

Moreover, most researchers have studied the corresponding properties of Cu/Ar nanofluids using MD methods, yet Ar is still not commonly used in industry and practical engineering applications. In this work, rutile-TiO_2 (r-TiO_2) /water nanofluids are selected as the research object. Using non-equilibrium molecular dynamics (NEMD) [30] approach based on the Fourier law, the thermal conductivity of TiO_2 (r-TiO_2)/water nanofluids is studied considering different volume fractions. The ordered layer structure as a shell is examined, and then its influence is surveyed by calculating the nanofluid number density and radial distribution function (RDF). Overall, comparison to the equilibrium molecular dynamics (EMD) approach, NEMD considers the influence of heat flux and avoids the generation of temperature gradients. This leads to more stable simulation system [31].

2. Modeling and Simulation

In general, the solid particle size utilized in this study to make nanofluids is between 10 and 100 nm. However, it is difficult and unrealistic to simulate the actual size of nanofluids with molecular dynamics (MD) [32], as the actual system is large and complex. Nevertheless, the MD method is a practical numerical simulation approach, that is based on Newtonian mechanics to simulate the motion of molecular systems. The method can evaluate the motion state of atoms in the model system through numerical simulations. In this regard, the mass and velocity of the atoms are calculated in the simulation system using Eq. (1) [33].

$$m_i \frac{dv_i}{dt} = F_{ij} = \nabla \varphi_{ij} \quad (1)$$

In Eq. (1), m_i and v_i are the mass and velocity of the atom, respectively. F_{ij} is the vector sum of all the interaction forces between atoms i and j. $\nabla \varphi_{ij}$ is the gradient of the potential function.

In addition, the thermal conductivities of TiO_2/water nanofluids were calculated using the large-scale atomic/molecular massively parallel simulator (LAMMPS) package, which is an open-source MD code. The MD simulation calculation provides microscopic information about the simulated system. Then, the utilized ensemble converts the related parameters calculated from MD in the microscopic state into macroscopic properties through statistical physics [34]. In this work, all simulations were carried out in canonical (NVT) and microcanonical (NVE) ensembles. A simulation box with 60Å×60Å×60Å dimensions was used to release water molecules. A TiO_2 nanocluster from materials studio (MS) was placed in the middle of the simulation box and was surrounded by water molecules. The visualization

tool OVITO was used to aid in the visualization and analysis of the atomistic simulation data obtained from the LAMMPS calculations [35].

Moreover, TiO_2 nanoclusters were set as spheres with radii of 8 and 10.1 Å. The SPC water molecular model was applied in the simulations. The number density of water molecules was calculated using Eq. (2) [14] and found to be 33.3 nm^{-3}, considering a density of 1000 kg/m^3.

$$n = {}^{N}/_{V} \tag{2}$$

In the above equation, N and V are the number of water molecules and volume of the calculated region, respectively. n indicates the quantity of water molecules in the studied region. Tab. 1 presents the detailed characteristics of TiO_2 nanoparticles. The SPC water model and the TiO_2 nanocluster model are shown in Fig. 1. Fig. 2 (a) shows the structure of TiO_2 nanoparticles and water molecules, as well as the initial position of TiO_2 nanocluster, which was set into the simulated box, considering volume fractions of 1.0 vol% and 2.0 vol%. Additionally, Fig. 2 (b) depicts a schematic of the simulation box of TiO_2 nanofluids using NEMD.

Tab. 1. Detailed characteristics of TiO_2 nanoparticles

Nanoparticles	Density g/cm^3	Specific heat $kJkg^{-1}K^{-1}$	Thermal conductivity $Wm^{-1}K^{-1}$
TiO_2	4.22	0.71	8.48

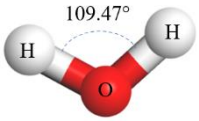

(a) SPC water molecular

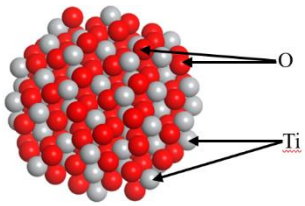

(b) TiO_2 nanocluster

Fig. 1. Illustration of models

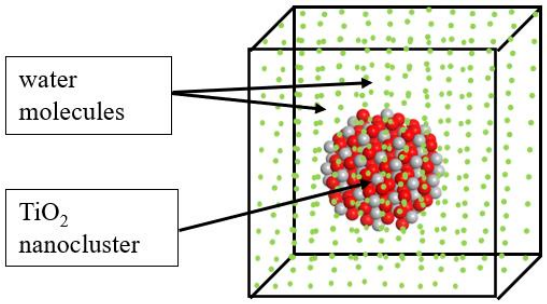

(a) Initial position of TiO_2 nanocluster

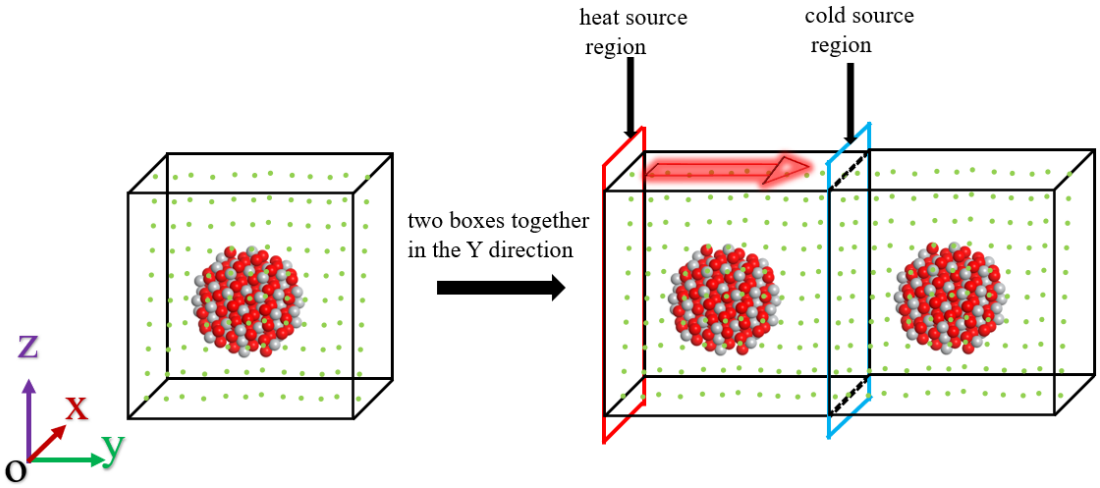

(b) Simulation box

Fig. 2. Schematic of the simulation using NEMD

The interatomic potentials between Ti-O, Ti-Ti, O-O, and Ti-O_w were modeled using the Matsui-Akaogi (MA) potential [36], as follows:

$$U(r_{ij}) = A_{ij}\exp\left(-\frac{r_{ij}}{\rho_{ij}}\right) - \frac{C_{ij}}{r_{ij}^6} + \frac{q_i q_j}{r_{ij}} \tag{3}$$

In Eq. (3), $U(r_{ij})$ represents the interatomic potential, and r_{ij} represents the distance between atoms i and j. The atomic charges of the oxygen and titanium are -1.098**e** and +2.196**e**, respectively. The other parameters $A_{ij}, \rho_{ij}, C_{ij}$ used by the MA potential function are shown in Tab. 2.

Tab. 2. Interaction parameters for the Matsui-Akaogi Force Field on TiO_2 and water oxygen

i-j	A_{ij} (kcal·mol^{-1})	ρ_{ij} (Å)	C_{ij} (kcal·mol^{-1} Å^6)
Ti-O	391,049.1	0.194	290.331
Ti- Ti	717,647.4	0.154	121.067
O-O	271,716.3	0.234	696.888
Ti-O_W	28,593.0	0.265	148.000

O_w: O in water.

In the SPC water molecular model, the interatomic potentials between O_w-O_w, H-H, and O_w -H were modeled using the Lennard-Jones (*L-J*) potential [31], as follows:

$$\begin{aligned} U(r_{ij}) &= 4\varepsilon_{ij}\left[\left(\frac{\sigma_{ij}}{r_{ij}}\right)^{12} - \left(\frac{\sigma_{ij}}{r_{ij}}\right)^{6}\right] \quad r_{ij}<r_c \\ U(r_{ij}) &= 0 \qquad\qquad\qquad\quad r_{ij}>r_c \end{aligned} \tag{4}$$

In Eq. (4), r_{ij} is the distance between atoms i and j. σ_{ij} and r_{ij} represent the energy and length scales, respectively. r_c is the cutoff distance, selected as 1.0 nm in this study for all intermolecular interactions. The interatomic potentials between O-O_w were modeled using the *L-J* potential [37]. The interaction between hydrogen atoms is neglected because of their very small mass. This means that the interaction between TiO_2 and water molecules is mainly based on the interaction between Ti, O atoms, and water oxygen.

During simulations, the time step was set to 1 fs in the NEMD simulation box, and the

long-range Coulomb forces were calculated to reflect the long-range interactions of the molecules. To reduce the effect of the simulated box size, periodic boundary conditions were set in the *x*, *y* and *z* directions of the considered system. To avoid any impact of the initial state on the simulation results, the model was completely relaxed under canonical ensemble (NVT) and microcanonical ensemble (NVE) for 100,000 steps. This allows for achieving stable temperature and energy conditions. Then, the same energy amount was added to the cold source and heat source regions, and the simulation box ran for 70,000 steps in NVE to generate a stable temperature gradient and heat flow parallel to the *y*-axis. Finally, the NEMD simulation box ran for another 100,000 steps to calculate the parameters of TiO_2/water nanofluids in NVE.

Implementing the above steps, the heat flux rate Φ and the temperature gradient values in the *y*-direction dt/dy can be obtained. Using these, the thermal conductivity λ can be calculated using Fourier's thermal conductivity law, combining Eqs. (5) and (6).

$$q_y = \frac{\Phi}{2(l_x \cdot l_z)} \tag{5}$$

$$q_y = -\lambda \frac{dt}{dy} \tag{6}$$

where Φ is the heat flux rate of the added cold or heat source. As, the added energy Φ will flow to both sides of the simulated box, Φ needs to be divided by 2 in Eq. (5). l_x and l_z represent the lengths of the simulation box on the *x* and *z*-axes, respectively. $l_x \cdot l_z$ represents the area perpendicular to the heat flux. q_y denotes heat flux density.

Fig. 3 shows the evolution of the temperature, kinetic energy, potential energy, and total energy of the system considering a temperature range of 303-333 K. It is noted that the system is in equilibrium within less than 100,000 steps in all the considered cases. Therefore, the system is considered stable before calculating the thermal conductivity by running 100,000 steps under the NVT and NVE ensembles.

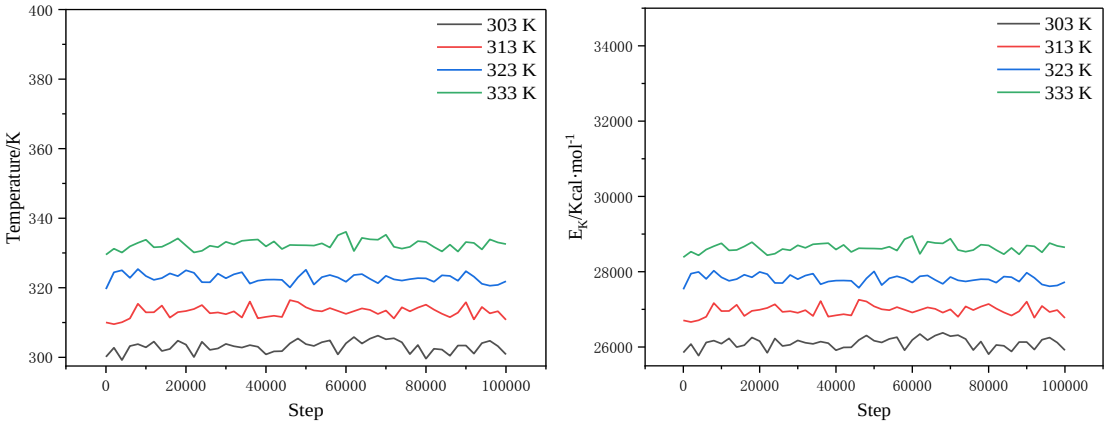

(a) **Temperature** (b) **Kinetic energy**

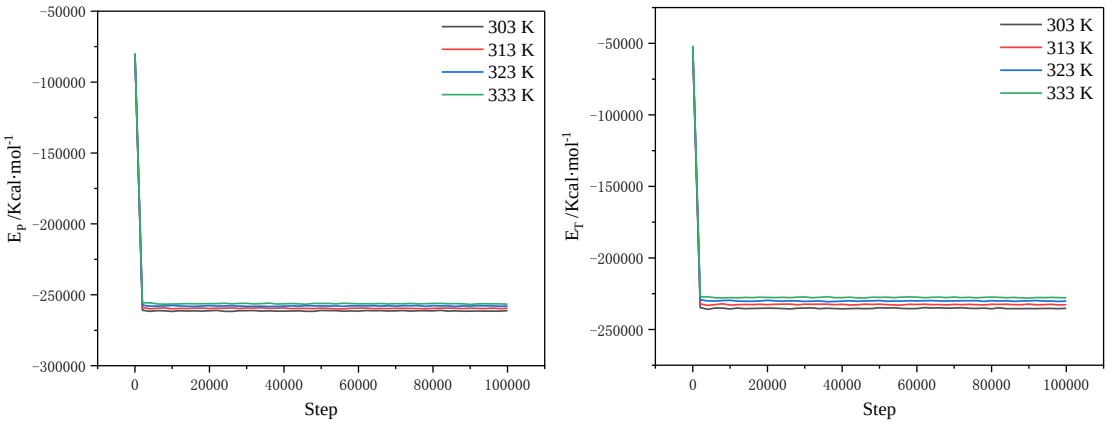

(c) **Potential energy** (d) **Total energy**

Fig. 3. Variations with steps, at volume fractions of 1.0 vol%.

3. Results and discussion

3.1. Validation of methods

Before calculating the thermal conductivity of the TiO_2/water nanofluid, the accuracy and stability of the simulation system were evaluated, considering a pure water system using the NEMD method. The validation results are presented in Fig. 4.

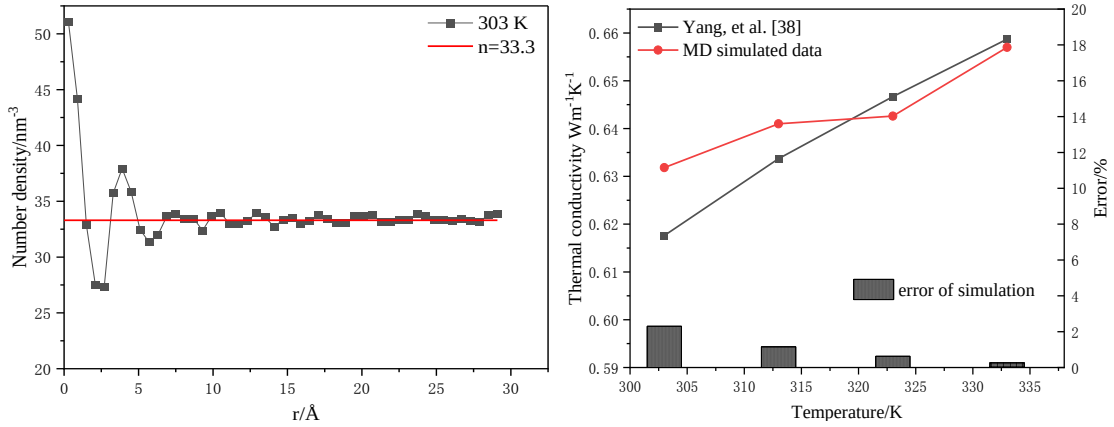

(a) **Number density** (b) **Thermal conductivity**

Fig. 4. Comparison of the simulation data and standard data from the literature [38].

Fig.4 shows the number density at 303 K in NEMD simulations and a comparison of the thermal conductivity data obtained in the present study and that reported in the literature. In the conducted simulations (Fig. 4 (a)), the number density is found to gradually converge to a constant value at 303 K, which is close to the standard value of 33.3/nm^3. As shown in Fig. 4 (b), the simulated data is found to be very close to the experimental data reported by Yang et al. [38]. The maximum error between the simulated values and the literature results is about 2.3% in the temperature range of 303-333 K. This finding verifies the reliability of the model established in this work.

3.2 Analysis of thermal conductivity

Macroscopically, the thermal conductivity increases with the increase in volume fraction. It was found that the increase in the volume fraction from 1% to 2% at 303 K resulted in an increase in the effective thermal conductivity ($\lambda_{eff} = \lambda_{nf}/\lambda_{bf}$) from 1.027 and 1.042, respectively. In other words, the thermal conductivity of the nanofluid was 2.7% and 4.2% higher than that of the base liquid under the same conditions. Figs. 5 (a) and (b) show the nanofluid's thermal conductivity λ_{nf} and effective thermal conductivity λ_{eff}obtained from simulations at a volume fraction of 1.0 vol%. It can be observed from Fig. 5 that the thermal conductivity of TiO_2/water nanofluids increases with an increase in temperature. The reason for the obvious enhancement in thermal conductivity at higher temperatures is attributed to the increase in the intense Brownian motion and interfacial potential of atoms and molecules [39].

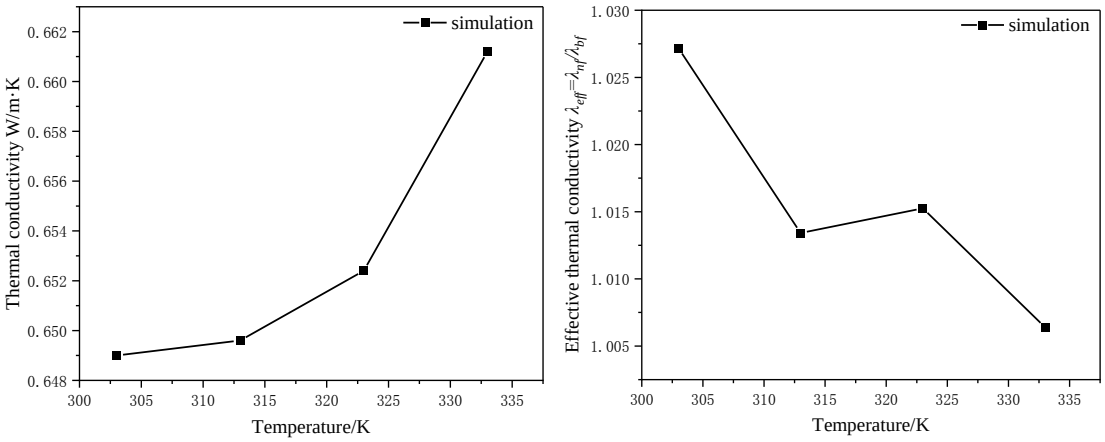

(a) Thermal conductivity **(b) Effective thermal conductivity**

Fig. 5. The thermal conductivity obtained from simulations at 1.0 vol%.

3.3. The function of the nano layer in the enhancement of TiO_2/water nanofluid thermal conductivity

The relationship between the nanolayer and heat transport, especially in terms of enhancing thermal conductivity, needs to be clarified. To evaluate whether the nanolayer can improve heat transport, the mechanism of enhancement of the nanofluids' thermal conductivity is examined and discussed with reference to RDF and, microscopic parameters such as nanolayer thickness and number density. The RDF function is a radial distribution function, denoted by *g*(r). The RDF represents the probability of finding an atom at a given distance away from the central atoms [40], and the number density shown in Eq. (2) is defined as the number of particles or substances per unit volume.

Fig. 6 shows the variation in the number density and *g*(r) with the change in the atomic distance *r* considering 1.0 vol% and 2.0 vol%. It can be seen from Fig. 6 that the number density and RDF function exhibited similar trends at different volume fractions. The number density distribution of water molecules around the TiO_2 central nanosphere is shown in Fig. 6 (a). As shown in the figure, at the beginning, the number density changes periodically with the atomic distance. Then, with the increase in the distance *r*, the number density approaches

a fixed value of 33.3 nm^{-3} (the number density of pure water). This indicates that the central nanosphere has a range of effects on the surrounding water molecules of about 0-0.5 nm, as shown in Fig. 6 (a). The first peak obtained for the number density is the strongest, with about 50nm^{-3}. This is followed by a second peak of about 38 nm^{-3}, while the rest of the peaks can be neglected. This result is consistent with the findings reported by Heyhat [37]. So, two distinct interfacial layers are formed around the central nanosphere.

Comparing Figs. 6 (b) and (c), the trend of g(r) is found to be similar at different volume fractions. In the range of 0-0.5 nm away from the TiO_2 central nanosphere surface, two obvious peaks are highlighted. This indicates that the probability of O_w appearing near Ti and O atoms is higher. Moreover, it is evident that the fluctuation of RDF is similar to that of the number density. If the shape is relatively sharp, it indicates that the number density is much higher than the average density within a specific area [41].

In addition, a larger value of the number density, or g(r) denotes a denser distribution of water molecules in the interfacial nanolayer, similar to the solid-like water molecular layer. In connection with this, Keblinski et al. [42] reported that the arrangement of liquid molecules is more ordered in such a layer. It is well known that solids possess better heat transfer properties compared to liquids. Thus, liquid layering at the interface of the nanoparticle would be expected to lead to higher thermal conductivity. Fig. 7 shows the schematic structure of two typical interfacial nanolayers around the center nanoparticle, obtained using OVITO. It is shown that a high heat conduction channel (center nanoparticle-interfacial nanolayers-random liquid molecules) is formed. Some studies have characterized the heat conduction channel as a thermal bridge [43].

As shown in Fig. 6 (a), the thickness of the first and second interfacial nanolayers is about 0.5 nm for TiO_2/water. According to the numerical density and RDF function, it noted that the density of water molecules is much higher than the density of the base liquid in the range of 0-0.5nm. At the same temperature of 333K, compared with pure water, the thermal conductivity of nanofluids has increased, and a clear solid-like nano layer can be observed around the nanoparticles. Therefore, the nanolayer plays a certain role in increasing the thermal conductivity of nanofluids.

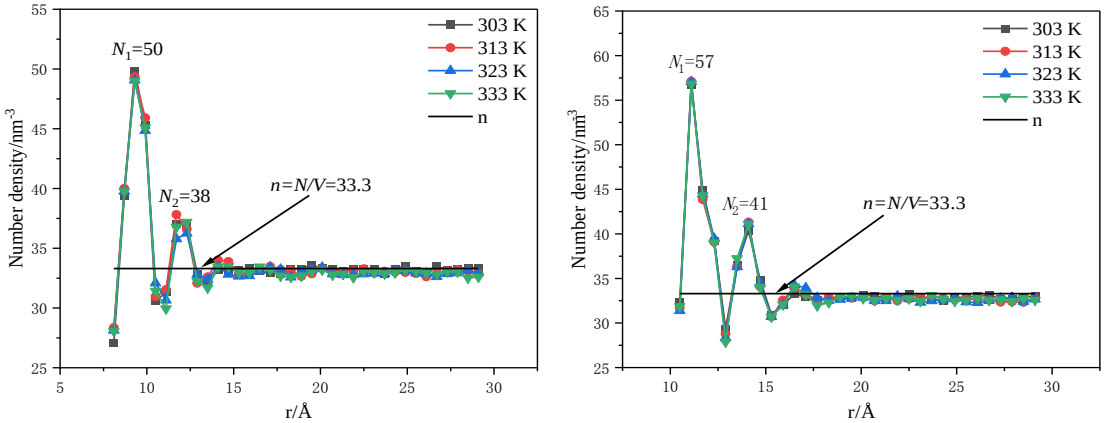

(a) Number density

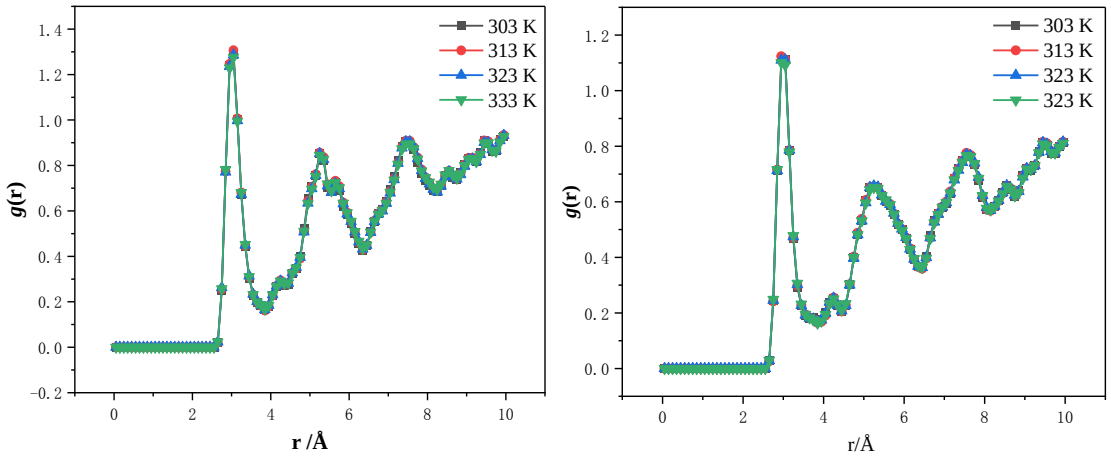

(b) *g*(r), of O-O_w

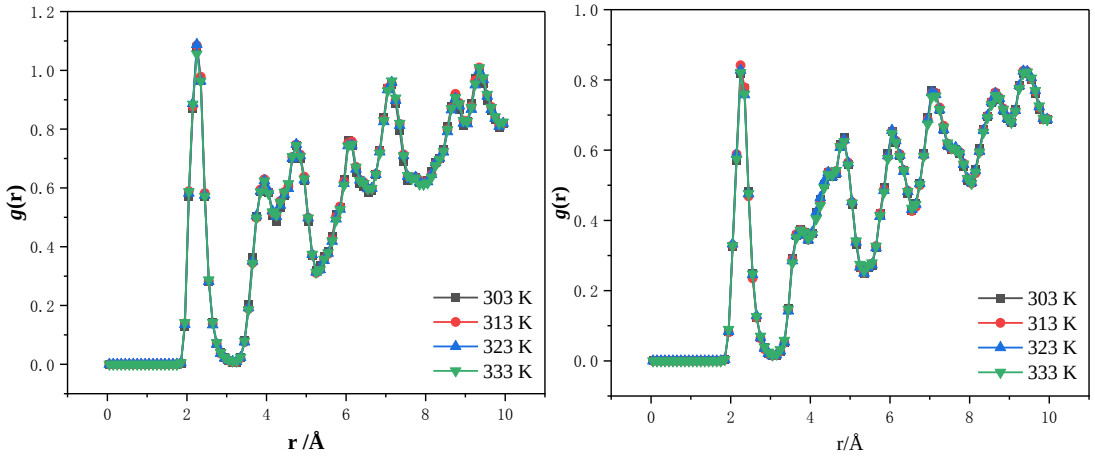

(c) *g*(r), of Ti-O_w

Fig. 6. Variations with the change in atomic distance at (left) 1.0 vol% and (right) 2.0 vol%.

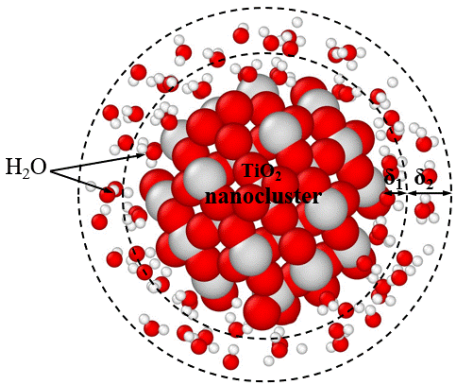

Fig. 7. Microscopic structure of the interfacial layer by OVITO.

4. Conclusions

In this study, a simulation model was established to estimate the thermal conductivity of TiO_2/water nanofluids for volume fractions of 1.0% and 2% of TiO_2. The thermal conductivity enhancement in nanofluids was described and evaluated considering the RDF,

the number density and nanolayer thickness. Based on the obtained results, the main conclusions that can be drawn from this study are as follows:

1. By considering the numerical simulations, it can be seen that the thermal conductivity of TiO_2/water nanofluids increases with an increase in temperature and volume fraction. A clear solid-like nanolayer (about 0.5 nm) can be observed around the nanoparticles.
2. The influence of volume fraction and temperature on number density and nanolayer thickness is relatively small.
3. In the process of heat transfer from the nanoparticles to the water molecules, the nanolayer acts as a connection. Regarding the increase in thermal conductivity of nanofluids, the nanolayer plays a certain role.

Due to the fact that the number density is less affected by temperature under the same volume fraction, there is still a need to study the interaction between the surface of TiO_2 nanocluster and water molecules.

Acknowledgment

This work was supported by the National Natural Science Foundation of China (No. 51966005) and the Yunnan Fundamental Research Projects (No. 202101AT070120. 202301AT070469).

References

[1] Karabulut, K., Heat transfer increment study taking into consideration fin lengths for CuO-water nanofluid in cross flow-impinging jet flow channels, *Therm. Sci. 27* (2023) 4345-4360. doi.org/10.2298/TSCI221203035K.

[2] Huang, H., *et al*., Study of a novel ternary second-order viscosity model on Al_2O_3-water nanofluid, *Therm. Sci. 27* (2023) 4223-4234. doi.org/10.2298/TSCI220926064H.

[3] Shen, B., *et al*., Application of Nanofluids in Minimum Quantity Lubrication Grinding, *Tribol. Trans. 51* (2008) 730-737. doi.org/10.1080/10402000802071277.

[4] Tian, S., *et al*., Using perceptron feed-forward Artificial Neural Network (ANN) for predicting the thermal conductivity of graphene oxide-Al_2O_3/water-ethylene glycol hybrid nanofluid, *Case Stud. Therm. Eng. 26* (2021) 101055. doi.org/10.1016/j.csite.2021.101055.

[5] Choi, S.U.S., Eastman, J.A., Enhancing thermal conductivity of fluids with nanoparticles, Argonne National Lab. (ANL), Argonne, IL (United States), 1995, https://www.osti.gov/biblio/196525.

[6] Ilyas, S.U., *et al*., Stability and thermal analysis of MWCNT-thermal oil-based nanofluids, *Colloids and Surfaces A: Physicochemical and Engineering Aspects*. *527* (2017), pp. 11-22. doi.org/ 10.1016/j.colsurfa.2017.05.004.

[7] Wang, X.Q., Mujumdar, A.S., A review on nanofluids-part I: theoretical and numerical investigations, Braz. J. *Chem. Eng*. *25* (2008), pp. 613-630, doi.org/10.1590/S0104-66322008000400001.

[8] Kazem, H.A., *et al*., Effect of CuO-water-ethylene glycol nanofluids on the performance of photovoltaic/thermal energy system: an experimental study, *Energy Sources Part Recovery Util. Environ. Eff. 44* (2022) 3673-3691. doi.org/10.1080/15567036.2022.2070305.

[9] Kazem, H.A., *et al*., Effect of Temperature on the Electrical and Thermal Behaviour of a Photovoltaic/Thermal System Cooled Using SiC Nanofluid: An Experimental and Comparison Study, *Sustainability. 14* (2022)

11897. doi.org/10.3390/su141911897.

[10] Yang, L., Du, K., A comprehensive review on heat transfer characteristics of TiO_2 nanofluids, *International Journal of Heat and Mass Transfer*. *108* (2017), pp. 11-31, doi.org/10.1016/j.ijheatmasstransfer.2016.11.086.

[11] Moradi, A., *et al*., Effects of temperature and volume concentration on thermal conductivity of TiO_2-MWCNTs (70-30)/EG-water hybrid nano-fluid, *Powder Technology*. *362* (2020), pp.578-585, doi.org/10.1016/j.powtec.2019.10.008.

[12] Kazemi, I., *et al*., A novel comparative experimental study on rheological behavior of mono & hybrid nanofluids concerned graphene and silica nano-powders: Characterization, stability and viscosity measurements, *Powder Technology*. *366* (2020), pp. 216-229, doi.org/10.1016/j.powtec.2020.02.010.

[13] Barnoon, P., *et al*., Two phase natural convection and thermal radiation of Non-Newtonian nanofluid in a porous cavity considering inclined cavity and size of inside cylinders, *Int. Commun. Heat Mass Transf. 108* (2019) 104285. doi.org/10.1016/j.icheatmasstransfer.2019.104285.

[14] Zhai, Y., *et al*., Determination of heat transport mechanism using nanoparticle property and interfacial nanolayer in a nanofluidic system, *Journal of Molecular Liquids*. *344* (2021) 117787, doi.org/ 10.1016/j.molliq.2021.117787.

[15] Abareshi, M., *et al*., characterization and measurement of thermal conductivity of Fe_3O_4 nanofluids, *Journal of Magnetism and Magnetic Materials*. *322* (2010), pp.3895-3901, doi.org/10.1016/j.jmmm.2010.08.016.

[16] Patel, H.E., *et al*., Thermal conductivities of naked and monolayer protected metal nanoparticle based nanofluids: Manifestation of anomalous enhancement and chemical effects, *Applied Physics Letters*. *83* (2003), pp. 2931-2933, doi.org/10.1063/1.1602578.

[17] Zhang, H., *et al*., The changes induced by pH in TiO_2/water nanofluids: Stability, thermophysical properties and thermal performance, *Powder Technology*. *377* (2021), pp. 748-759, doi.org/10.1016/j.powtec.2020.09.004.

[18] Moosavi, M., *et al*., A. Youssefi, Fabrication, characterization, and measurement of some physicochemical properties of ZnO nanofluids, *International Journal of Heat and Fluid Flow*. *31* (2010), pp. 599-605, doi.org/10.1016/j.ijheatfluidflow.2010.01.011.

[19] Zhang, X., *et al*., Experimental Study on the Effective Thermal Conductivity and Thermal Diffusivity of Nanofluids, *Int J Thermophys*. *27* (2006), pp. 569-580, doi.org/10.1007/s10765-006-0054-1.

[20] Saleh, R., *et al*., Titanium dioxide nanofluids for heat transfer applications, Experimental Thermal and Fluid Science. *52* (2014), pp.19-29, doi: 10.1016/j.expthermflusci.2013.08.018.

[21] Yu, W., Choi, S.U.S., The role of interfacial layers in the enhanced thermal conductivity of nanofluids: A Renovated Maxwell Model, *Journal of Nanoparticle Research*. *5* (2003), pp. 167-171, doi.org/10.1023/A:1024438603801.

[22] Li, L., *et al*., An investigation of molecular layering at the liquid-solid interface in nanofluids by molecular dynamics simulation, *Physics Letters A. 372* (2008), pp. 4541-4544, doi.org/10.1016/j.physleta.2008.04.046.

[23] Suganthi, K.S., *et al*., Liquid-layering induced, temperature-dependent thermal conductivity enhancement in ZnO-propylene glycol nanofluids, *Chemical Physics Letters*. *561-562* (2013), pp. 120-124, doi.org/10.1016/j.cplett.2013.01.044.

[24] Cui, W., et al., Molecular dynamics simulation on the microstructure of absorption layer at the liquid-solid interface in nanofluids, *International Communications in Heat and Mass Transfer*. *71* (2016), pp. 75-85, doi.org/10.1016/j.icheatmasstransfer.2015.12.023.

[25] Choi, S.U.S., *et al*., Anomalous thermal conductivity enhancement in nanotube suspensions, *Applied Physics Letters*. *79* (2001), pp. 2252-2254, doi.org/10.1063/1.1408272.

[26] Li, L., *et al*., Molecular dynamics simulation of effect of liquid layering around the nanoparticle on the

enhanced thermal conductivity of nanofluids, *J Nanopart Res*. *12* (2010), pp. 811-821, doi.org/10.1007/s11051-009-9728-5.

[27] Wang, X., Jing, D., Determination of thermal conductivity of interfacial layer in nanofluids by equilibrium molecular dynamics simulation, *Int. J. Heat Mass Transf. 128* (2019) 199-207. doi.org/10.1016/j.ijheatmasstransfer.2018.08.073.

[28] Jin, X., *et al*., Effect of interfacial layer around core-shell nanoparticles on thermal conductivity of nanofluids, *Powder Technol. 429* (2023) 118945. doi.org/10.1016/j.powtec.2023.118945.

[29] Jin, X., *et al*., The most crucial factor on the thermal conductivity of metal-water nanofluids: Match degree of the phonon density of state, *Powder Technol. 412* (2022) 117969. doi.org/10.1016/j.powtec.2022.117969.

[30] Sedighi, M., Mohebbi, A., Investigation of nanoparticle aggregation effect on thermal properties of nanofluid by a combined equilibrium and non-equilibrium molecular dynamics simulation, *Journal of Molecular Liquids*. *197* (2014), pp. 14-22, doi.org/10.1016/j.molliq.2014.04.019.

[31] Chen, W., *et al*., A molecular dynamic simulation of the influence of linear aggregations on heat flux direction on the thermal conductivity of nanofluids, *Powder Technology*. *413* (2023) 118052, doi.org/org/10.1016/j.powtec.2022.118052,

[32] Milanese, M., *et al*., An investigation of layering phenomenon at the liquid–solid interface in Cu and CuO based nanofluids, *International Journal of Heat and Mass Transfer*. *103* (2016), pp. 564-571, doi.org/ 10.1016/j.ijheatmasstransfer.2016.07.082.

[33] Wang, R., *et al*., Investigation of the aggregation morphology of nanoparticle on the thermal conductivity of nanofluid by molecular dynamics simulations, *International Journal of Heat and Mass Transfer*. *127* (2018), pp.1138-1146, doi.org/10.1016/j.ijheatmasstransfer.2018.08.117.

[34] Bai, S., *et al*., Numerical simulation of thermal conductivity of rutile titanium dioxide film, J*ournal of Liaoning Normal University (Natural Science Edition), 45*(1) (2022), pp.31-37

[35] Stukowski, A., Visualization and analysis of atomistic simulation data with OVITO–the Open Visualization Tool, *Modelling Simul. Mater. Sci. Eng*. *18* (2009) 015012, doi.org/10.1088/0965-0393/18/1/015012.

[36] English, N.J., *et al*., Hydrogen bond dynamical properties of adsorbed liquid water monolayers with various TiO_2 interfaces, *Molecular Physics*. *110* (2012), pp.2919-2925, doi.org/10.1080/00268976.2012.683888.

[37] Heyhat, M.M., *et al*., Molecular dynamic simulation on the density of titanium dioxide and silver water-based nanofluids using ternary mixture model, *Journal of Molecular Liquids*. *333* (2021) 115966, doi.org/10.1016/j.molliq.2021.115966.

[38] Yang, S., Tao, W., Heat Transfer, Higher Education Press, Beijing, China, 2019.

[39] Borzuei, M., Baniamerian, Z., Role of nanoparticles on critical heat flux in convective boiling of nanofluids: Nanoparticle sedimentation and Brownian motion, *International Journal of Heat and Mass Transfer*. *150* (2020) 119299, doi.org/10.1016/j.ijheatmasstransfer.2019.119299.

[40] Li, Y. *et al*., Using molecular dynamics simulations to investigate the effect of the interfacial nanolayer structure on enhancing the viscosity and thermal conductivity of nanofluids, *International Communications in Heat and Mass Transfer*. *122* (2021) 105181, doi.org/10.1016/j.icheatmasstransfer.2021.105181.

[41] Zhang, S., *et al*., Summary of methods for structural analysis and characterization in molecular modeling, *J. Yanshan Univ*. *39* (3) (2015), pp. 213-220.

[42] Keblinski, P., *et al*., Mechanisms of heat flow in suspensions of nano-sized particles (nanofluids), *International Journal of Heat and Mass Transfer*. *45*(4) (2002), pp. 855-863.

[43] Gupta, M., *et al*., A review on thermophysical properties of nanofluids and heat transfer applications, *Renewable and Sustainable Energy Reviews*. *74* (2017), pp. 638-670, doi.org/10.1016/j.rser.2017.02.073.

RECEIVED DATE: 10.10.2023
DATE OF CORRECTED PAPER: 11.11.2023
DATE OF ACCEPTED PAPER: 19.12.2023.